7.9 - 1 0 1 0 6.
CR - 158080

NSG 5014

An Investigation of Vegetation and Other Earth Resource/
Feature Parameters Using Landsat and Other Remote Sensing Data

A. Landsat

B. Remote Sensing of Volcanic Emissions

Semi-Annual Status Report (#9)

July 1 to December 31, 1978

Dartmouth College

Hanover, NH 03755

Principal Investigators:

Richard W. Birnie

Richard E. Stoiber

Researchers:

Emily Bryant

Joseph Francica

Lawrence Malinconico

Dartmouth College

Semi-Annual Status Report - NSG 5014 - December 31, 1978

This report covers activities of the Landsat Sensing
Research Group (Earth Resources) and of the Volcanic Gas Sensing
Research Group (Planetary Science) which work in collaboration
with the Goddard Institute for Space Studies, New York,
Dr. Robert Jastrow, Director and Technical Officer for this
project.

A.   Landsat

The Dartmouth Landsat Research Group continued application
studies for Landsat data under the general category of analysis
of vegetation cover, especially forestry and geobotany, that
is, the effects of soil/earth mineral content on vegetation.

1.   Agricultural Crop Studies. No research activities in
period. (No funds allocated.)

2.   Forestry (Emily Bryant). This work includes the effort
of Ms. Bryant and her student assistants, in collaboration with
A.G. Dodge, Area Forester, Cooperative Extension Service,
University of New Hampshire, whose services are furnished under
a task order to UNH by Dartmouth.

We have continued in both lines of research mentioned
in the previous report: clearcuts, consistency.

A.   Clearcuts -- Field checked and took photos of
recent clearcuts in northern New Hampshire in August. Photos
used in a prototype "photo-key" -- a visual aid to explain

computer classification of clearcuts to field personnel and researchers. Brought the clearcut classification to a point where we are ready to work with subsequent Landsat passes.

B. Consistency -- Our assistant worked on getting consistent classification of an area in northern New Hampshire in three summer Landsat passes, 1973, 1975, and 1976. Preliminary results with the 1973 and 1975 data show acreages of major forest types (softwood, mixed wood, and hardwood) were within about 15 - 20% of each other on test areas of sizes ranging from 20,000 to 400,000 acres. Checked our softwood training area to see if it is still valid to use with 1978 data.

Completed printout of Franklin County, Massachusetts. It showed more softwood than was indicated in a classification of the same area done by Bendix.

We have also worked on a project to test the atmospheric simulations which Richard Kiang has developed. This involves classifying a 720,000 pixel (826,000 acre) area, and reclassifying it 6 times with 6 different atmospheric perturbation simulations.

Spreading the word, maintaining contacts with remote sensing and forestry world.

A. Spreading the Word -- Dodge and/or Bryant gave talks/ lectures as follows:

- Squam Lake Science Center, Holderness, N.H.

  corporation meeting, July 22.

- Meeting of the New England - St. Lawrence Valley Association of Geographers, October 20.

- Annual Meeting of all Cooperative Forest Management Supervisors in the Northeast (20 states), September 19.

- Remote Sensing class, Dartmouth, November 14.

- Submitted two presentation summaries for poster session at 13th International Remote Sensing Symposium at ERIM, University of Michigan, April, 1979 (Enclosures 1 & 2).

B. Contacts

- Went to Ottawa, Canada and visited Canada Centre for Remote Sensing and the Canadian Forest Fire Research Institute, September 5-7. Compared their techniques with ours using our computer compatible Landsat tapes.

- Went to meeting of the Remote Sensing Group of northern New England, September 28-29. Accepted some responsibility for the next annual program.

- Talked with Jack Estes of NASA Headquarters, October 1.

- Went to GISS and talked with people up from NASA; also exchanged ideas with people at GISS, November 8-9.

- Discussed Landsat data classification techniques with Ben Merembec from ORSER, Penn State.

- Maintained contact with Darrel Williams of GSFC by telephone.

3. <u>Land Use</u>. No research activities in period. (No funds allocated).

4. <u>Water Quality</u>. No research activities in period. (No funds allocated.)

5. <u>Mineral Resources</u>. Work under this heading is undertaken by Professors Birnie and Stoiber, with Joseph Francica and student assistants.

a) Airborne multispectral scanner experiments were undertaken in the fall of 1978 over the American River copper prospect in Washington State. The deposit is overlain by a dense fir forest with some tamarack. The purpose of these experiments is to see if the presence of the known mineral deposit is manifested as a geobotanically anomaly that can be detected by remotely obtained high resolution reflected radiance data. These data have been collected and are being analyzed now.

The spectral characteristics of the fir forest will be compared with those of a lodgepole pine forest collected over the Heddleston porphyry copper molybendum deposit in Montana in 1975. A geobotanical anomaly was detected in the Heddleston data. If prospecting for ore deposits using airborne multispectral scanner data to detect geobotanical anomalies is to be universally applicable, the method must be tested at different types mineral deposits with different types of forest cover.

A classification algorithm for aircraft data has been developed. This classification discriminant is based on the observation in the Heddleston data that the mineralized spectra have higher reflected radiance values in the 0.67 μm region of the spectrum.

b) Landsat Data. A study of the northwestern Adirondack Mountain region has been undertaken using digital processing of Landsat data. The Landsat data is being used to attempt to map a complex metamorphic area of marbles and gneisses. These rock types are manifested on the surface by different surface covers and vegetation patterns. A map has been procduced but it is being improved by more careful attention to classification parameters. The GISS "fixed volume" classification is being used.

c) Application of Remote Sensing to Reconnaissance Geologic Mapping and Mineral Exploration. This paper by Prof. Birnie and Dr. Jon Dykstra (former graduate student) has been published in the Proceedings of the 12th International Symposium, Remote Sensing of the Environment (Enclosure 3, reprint).

B. Remote Sensing of Volcanic Emissions. This work was undertaken by Prof. Stoiber, Lawrence Malinconico, Technical Assistant Geoffrey Bratton and student assistants.

1) Data from aircraft SO_2 monitoring (COSPEC) in February 1978 was presented at a meeting of the GSA and of Canada (1978 Joint Meeting) in Toronto, October 28 and of the

American Geophysical Union in San Francisco in December 1978. This data is now being prepared for publication. (Abstracts at Enclosures 4 & 5).

2) Arrangements have been made to run another set of experiments on sulfur dioxide determination from the air similar to those of February 1978. This will be as before in cooperation with NCAR using the Queenaire in February 1980.

3) The Remotely Piloted Aircraft project was inactive because plans to visit, for a field trial, the optimum locality at Masaya, Nicaragua, were cancelled due to extreme political unrest in Nicaragua. Samples were collected on the ground at the Volcano San Miguel in El Salvador. These were used to further refine our analytical techniques for the determination of chlorine and sulfur dioxide in gases collected either by hand or by remotely piloted vehicles at fuming volcanic craters.

4) The hydrochloric acid monitoring project (GASPEC) moved ahead to the point the sensor is now performing in the laboratory. Tests will be run to determine how well and then further reduction of the noise will be attempted. This further work depends on hiring a new technician which is planned for early 1979.

5) Funding for a planned expedition to the Antaractic to do volcano research with Ohio State University personnel in December 1979 was denied by the NSF. We await copies of the reviewers comments before deciding our next move.

6) We expect to visit Mt. Etna once in 1979 to establish base levels of output of sulfur dioxide. A paper relative to premonitory increases in sulfur dioxide at Etna volcanic eruptions has been submitted for publication to Nature.

7) Work at both Kilauea and Mauna Loa Volcanoes in Hawaii has been stepped up. The first visit to Kilauea with the COSPEC was in January 1975. Very similar output of sulfur dioxide was recorded on our latest visit October 1978. At Mauna Loa in 1978 the output was at most a few tons per day. This visit was sponsored by this grant, the United States Geological Survey and the NOAA people. (See Trip Report, Malinconico, Stoiber September 29-October 17, 1978). Plans are in progress for the continuous monitoring of Kilauea for a month in July or August 1979 in collaboration with USGS. Further investigations of Mauna Loa will be instituted as part of our study of the major components of Hawaiian volcanic gases. We hope to study condensates of Hawaiian fumaroles during the coming summer. This will be a master's degree project for a Dartmouth student if present arrangements go forward. Since the Hawaiian volcanoes are genetically different from those of circumpacific and Kilauea is also likely to erupt every few years, the studies in Hawaii will be important in our overall program.

8) We were invited to give a paper relating the information regarding Hawaiian volcanic gases to the study planetary atmospheres. The information in the paper was perhaps reported somewhat prematurely but we took this opportunity to be represented in the JPL Symposium on Planetary Atmospheres in January 1979.

9) The immediate goal of our gas program is to determine the SO_2 output at different volcanoes and at different stages in volcanic activity. This requires the piecing together of innumerable pieces of data and will perhaps require some continuous monitoring for periods of a month or so at selected places. It is in this regard that we have chosen to monitor Kileauea. It appears that, at the present the state of our information, the output of sulfur dioxide during the various stages of activity, changes by the order of magnitude or more, where as the differences between several volcanoes at the same stage is decidedly less than half an order of magnitude. The goal, the overall pattern of volcanic emission at volcanoes of several kinds, will not be reached in a single year but will demand several years study. Our new Hawaiian work described above is another facet of this overall press for information that can be integrated into a world volcanic sulfur dioxide budget.

Small Forest Cuttings Mapped With Landsat Digital Data

by Emily Bryant, Arthur G. Dodge, Jr., and Martha Jean Eger

NASA Science Grant 5014 supports a cooperative project between the Goddard Institute for Space Studies, New York City, Cooperative Extension Service, University of New Hampshire, and Dartmouth College, Hanover, New Hampshire. Our goal is to produce useful forest information through computer classification of Landsat data. We have mapped forest types (hardwood and softwood) with some success. Forest types do not make up the entire picture, however. A forester also needs frequent updating on the location, size, and condition of harvested areas (cuttings) to manage his lands. We have thus turned our efforts toward mapping forest cuttings, specifically clearcuts in northern New Hampshire.

Using Landsat data of June 26, 1975 (scene 5068-14433), we developed a supervised classification of clearcut areas. A total of 60 cuts in northern New Hampshire were used as training and test areas. Cuts in this region range in size from 5 to 500 acres, commonly about 40 acres. Different stages of regrowth in the cuts had different signatures; we found we were able to distinguish five general age categories.

We provided public and private foresters with sample printouts of their land for evaluation. They were satisfied with the shape and location of the cuts. Accuracy of size compared to ground truth provided by field foresters was variable, but to quote one, "probably your figures are better than ours".

An essential part of mapping clearcuts is identifying changes from

year to year. This requires classification categories which are consistent from one Landsat pass to another. We are currently experimenting with the development of consistent forest categories for three Landsat passes over a base area with little change during the time of the passes. Difference in acreage estimates from the three passes in three forest categories was rarely more than 15% in selected 30,000 acre areas.

We feel that the capability to map clearcuts brings Landsat a step closer to being an operational part of current forest inventories and management activities.

A KEY FOR BETTER INTERPRETATION OF LANDSAT DIGITAL DATA

by

Arthur G. Dodge, Jr., Emily S. Bryant & Martha Jane Eger

Tools should be developed that increase accuracy, save time and improve or broaden the skills of people involved in remote sensing activities.

Keys are tools that have been used by photo interpreters for many years. They can be descriptive, pictorial , or both, in format. Their usefulness is only limited by the imagination of the creator or the ability of the user.

Adapting Landsat digital data into established inventory systems or applying satellite data for solving forest management problems has often been questioned by field users and potential users.

We have observed that one road block to more use of Landsat digital data is a lack of understanding, by the user, of what is being displayed on a printout or CRT screen. Another observation is that effective interpretation of Landsat data increases in direct proportion to correlation of that data with conditions in the field.

Field checking the interpretation or analysis of any remote sensing data is exacting, tedious, time consuming and expensive. It can also be fun or very un-comfortable. Historically, field checking time has become more limited due to financial restrictions and added new demands upon all users of remote sensing data.

We have developed a photo-digital key which graphically describes forestry field conditions and illustrates how these conditions are displayed on a Landsat digital printout. The key was developed while mapping forests in northern New Hampshire. We have been able to include in the key:

    Water
    Hardwood Forest
    Softwood Forest
    Mixed Wood Forest
    Clearcuts in hardwoods or mixed wood with five stages of forest regrowth
    Clearcuts in softwood forest

We believe that this key can be used to analyze Landsat data covering northern New England. Slight modification could adapt it to other areas of the Northeastern United States and Canada.

Advantages of this key are:

Introductory description of forest conditions for beginning data analysts.

More accurate interpretation of Landsat forest mapping before field checking.

Less field checking time needed.

A better way to describe Landsat forestry mapping to new users and

potential users.

NOTE: This is a joint project between the Cooperative Extension Service,
University of New Hampshire. Dartmouth College, and Goddard Institute
for Space Studies, New York, NY, under NASA Grant 5014.

Arthur G. Dodge, Jr. (Gibb) is employed by Cooperative Extension Service, University of New Hampshire, as an Area Forester and State Forestry Planner with headquarters in Conway, New Hampshire.

Emily S. Bryant is a Researcher employed by Dartmouth College, Hanover, New Hampshire and Goddard Institute of Space Studies, New York, NY.

Martha Jane Eger was employed as Research Assistant by Dartmouth College and Goddard Institute of Space Studies, and is now a graduate student in remote sensing at University of Kansas, Lawrence, KA.

APPLICATION OF REMOTE SENSING TO RECONNAISSANCE GEOLOGIC
MAPPING AND MINERAL EXPLORATION

Richard W. Birnie and Jon D. Dykstra
Department of Earth Sciences
Dartmouth College
Hanover, NH 03755

ABSTRACT

A method of mapping geology at a reconnaissance
scale and locating zones of possible hydrothermal
alteration has been developed. This method is based
on principal component analysis of LANDSAT digital
data and is applied to the desert area of the Chagai
Hills, Baluchistan, Pakistan. A method for airborne
spectrometric detection of geobotanical anomalies
associated with porphyry Cu-Mo mineralization at
Heddleston, Montana has also been developed. This
method is based on discriminants in the 0.67 μm and
0.79 μm region of the spectrum.

I. INTRODUCTION

This paper considers two applications of remote sensing to geology. The
first method uses computer processed LANDSAT digital data to map geology over
large areas of well exposed surface features. The second method employs a
high resolution airborne spectrometer to detect geobotanical anomalies asso-
ciated with Cu-Mo mineralization.

II. DIGITAL PROCESSING OF LANDSAT DATA

A computer algorithm for the classification of LANDSAT digital data has
been developed at Dartmouth College in cooperation with the Goddard Institute
for Space Studies, New York. This algorithm has been applied to the Chagai
Hills, which form an eliptical massif covering about 170 by 40 km in south-
western Pakistan (Figure 1). The region is well suited for a remote sensing
study because of its extreme aridity and near total lack of vegetation which
might otherwise contaminate the spectral signatures of the surface geology.
Furthermore, due to the rugged topography and limited access to interior
regions of the Chagai Hills, remote sensing is a cost and time efficient way
to gain information on the extent and distribution of surface geologic types.

The Chagai Hills are a predominantly igneous terrain. The major forma-
tion is the Sinjrani Volcanics which consists of over 1300 m of andesitic
flows, agglomerates, volcanic conglomerates, and pyroclastics with small
amounts of rhyolite and basalt (Hunting Survey, 1960). The intrusive rocks
in the Chagai Hills, the Chagai Intrusives, are divided into two groups: a
dark, main phase of granodiorite-quartz diorite composition and a lighter toned,
younger phase of granitic composition.

The Chagai Hills are believed by these authors to be an extension of the
Tethyian Suture Zone of Iran. Several porphyry occurrences are known in Iran
along the Suture Zone; the Saindak porphyry copper deposit lies west of the
Chagai Hills, and new prospects in the area between the Chagai Hills and
Saindak have been located using computer processing of LANDSAT digital data

(Schmidt and Bernstein, 1977). Several prospects are known to exist in the Chagai Hills and the possibility of additional occurrences is believed to be good.

The classification algorithm differentiates seven surface geologic types over the 5200 m^2 of the Chagai Hills. These include the bedrock units described above: 1) the Sinjrani Volcanics, 2) the granodiorite-quartz diorite phase of the Chagai Intrusives, and 3) the granitic phase of the Chagai Intrusives. Three unconsolidated surface units are also mapped and these include: 1) volcanic float derived from high standing Sinjrani Volcanics and often mantling low lying Chagai Intrusives, 2) dry wash deposits of clastic sediments, and 3) granitic talus localized arou high stands of Chagai granites. The last surface geologic type is zones of hydrothermal alteration, which are characterized by areas of subtle iron oxide staining created by weathering of sulfide minerals associated with phyllic and potassic alteration.

The classification of the digital data requires choosing control areas of the surface geologic types which are to be mapped. These were chosen on the basis of field and aerial photographic studies. The distribution of reflected radiances of pixels of a given control area type is represented by a "characteristic line" in the LANDSAT 4-dimensional color space. This "characteristic line" is a line parallel to the principal component of the data and passing through the center of gravity of the data. Examples of "characteristic lines" for hypothetical distributions of pixels within two control area types (A and B) are plotted in two dimensions in Figure 2. In the actual classification procedure, there is a 4-dimensional "characteristic line" for each control area type.

The LANDSAT color space can be sliced by lines of constant total reflected radiance representing the sums of the reflected radiance values in the four LANDSAT bands. These lines of constant total reflected radiance are shown as dashed lines in the 2-dimensional representation in Figure 2. These lines divide the color space into "slices" with slice #1 representing total reflected radiance values achieved only by control area type B; slice #2 includes total reflected radiance values of control areas A and B; and slice #3 contains only A. This slicing is equivalent to defining areas of overlap and non-overlap of the distribution of pixels as projected onto a line perpendicular to the lines of constant total reflected radiance. The LANDSAT 4-dimensional color space can be sliced in a similar manner to determine which control areas are to be considered possible classifications based on the total reflected radiance value of an unknown pixel. An unknown pixel need only be tested for possible classification with those control area types whose distribution of total reflected radiance values overlaps that of the unknown pixel.

The next discriminant in the classification procedure is based on an unknown pixel's distance from the "characteristic lines" of the individual control areas. These distances are measured on the perpendicular from the unknown pixel to the "characteristic line" (DEL_A or DEL_B in Figure 3). The separation of two "characteristic lines" is also calculated (DIF_{AB} in Figure 3). The likelihood of a given pixel's belonging to a control area type is quantified by calculating a "confidence value" defined as DIF/DEL. The "confidence value" is, therefore, directly proportional to the separation of the "characteristic lines" (DIF) and inversely proportional to the pixel's distance from the "characteristic lines" (DEL). Classification information in a single pixel is augmented by that of its neighbors by summing "confidence values" of a central pixel and its eight contiguous neighbors. The central pixel is classified as the control area with the highest summed "confidence value".

The above described classification procedure applies to reconnaissance

796

mapping of regional geology where each control area has a sufficiently large pixel population to establish a well defined "characteristic line". Known areas of hydrothermal alteration in the Chagai Hills provide only five pixels which satisfactorily represent the zones of potential mineralization. A reliable "characteristic line" cannot be calculated from so few datum points, so the classification of zones of possible hydrothermal alteration is based on individual pixel spectra. Pixels in the Chagai Hills that have spectral signatures exactly matching those of the known hydrothermal alteration pixels are classified as altered if they and at least two of their eight contiguous neighbors have hydrothermally altered signatures.

Every pixel in the Chagai Hills was classified by the above procedure, and a 1:48,000 scale map of surface geologic types was generated. This final LANDSAT geologic is too large to be included in the format of these proceedings; however, portions of this map will be shown and compared to portions of the 1:253,400 scale photo-geologic map of the Hunting Survey (1960). A portion of the Hunting photo-geologic map is shown in Figure 4a. This map distinguishes zones of Sinjrani Volcanics (SjV), volcanic float (Rec), and zones of Chagai Intrusive (ChI). The LANDSAT geologic map for the same area is shown in Figure 4b. The photo-geologic map does not differentiate the intrusive phases, but the satellite identifies the intrusive in this area as the older granodiorite-quartz diorite phase (ChI(a)). This classification agrees with our field studies. The agreement between the photo-geologic map and the LANDSAT map is seen to be good, particularly when the geologic interpretation based on our field observations is made that the area mapped as volcanic float (Rec) on the LANDSAT map is underlain by Chagai Intrusives. Another area of the Chagai Hills is shown in Figures 5a and 5b. The LANDSAT geologic map distinguishes two intrusive phases: 1) granite (ChI(b)) and 2) granodiorite (ChI(a)). The Hunting Survey's (1960) photo-geologic study did not separate these two phases, and showed the Chagai Intrusives as a single, undifferentiated unit (ChI). The dimensions of the granite shown in the LANDSAT map agree well with our field observations. Zones of possible hydrothermal alteration have been identified in regions of the Chagai Hills, and these zones will be the subject of upcoming field studies.

It should be emphasized that the entire 5200 km^2 of the Chagai Hills have not been field checked. The lack of detailed ground truth makes estimation of errors of omission and comission impossible. However, we draw a largely favorable qualitative comparison between our LANDSAT surface geologic map and the photo-geologic map of the Hunting Survey (1960). It should be further emphasized that a good deal of geologic information which is impossible to obtain from the LANDSAT mapping procedure described herein can be derived from conventional field techniques. However, we believe that this LANDSAT geologic mapping procedure offers a valuable method of reconnaissance geologic mapping. The main advantage is that it allows reconnaissance scale mapping of large regions at a fraction of the expense and man hours involved with conventional techniques. Another advantage over conventional photo-interpretation studies is the ability to make geologic discriminations on the basis of color. In addition, the objective nature of the machine processing decreases the possibility of subjective errors.

III. AIRBORNE SPECTROMETRIC DETECTION OF GEOBOTANICAL ANOMALIES

Where surface exposures of the geology are masked by vegetation, an airborne spectrometer has been used to detect geobotanical anomalies. These anomalies manifest the toxic effects of mineralization and thus may be used as targets in an exploration program. The airborne spectrometer used in this study was developed by William Collins and is described by Collins (1976). The instrument measures reflected radiance (mW/cm^2.sr) in the visible and near infrared region of the spectrum. The spectral band width is about

797

0.0014 µm. The instrument was mounted in a Rockwell Aero Commander 680-E and
flown at an elevation of about 600 m above the surface. The reflected ra-
diance was integrated over a surface area about 18 m square, and photographs
were taken every 10 spectra to permit a correlation of the reflected radiance
spectra with the ground surface.

The area chosen for this study is the Heddleston copper-molybdenum
porphyry deposit located about 50 km NW of Helena, Montana. The geology is
reported by Miller et al. (1973). The deposit is localized in a complex
series of tertiary quartz monzonite and quartz porphyry intrusives. These
prophyries intrude the Precambrian Spokane Formation of the Belt Series and
are cut by a Cretaceous (?) diorite sill. A broad 1.6 km^2 area of the in-
trusives shows sericitic, silicic, and argillic alteration. The mineraliza-
tion includes primary chalcopyrite and molybdenite with zones of supergene
chalcocite and covellite. Drilling has delineated zones of shallow to inter-
mediate depth mineralization (Figure 9), which are thinly covered by alluvium
and leached capping (Miller et al., 1973). Dense pure stands of lodgepole
pine (Pinus contorta) up to 25 m high cover much of the deposit.

The deposit was traversed by a series of flight lines that covered both
the mineralized and nonmineralized zones. Each flight line was about 2 km
long and included about 100 spectra, of which between 10 and 30 were of
lodgepole pine from the mineralized zones (Figure 9).

The first test was to determine if spectra known to be from the
mineralized zone were different from spectra from outside the mineralized
zone. Photos taken from the aircraft were used to isolate spectra of uniform-
ly dense lodgepole pine. Spectra that included areas of streams, roads, grass,
or nonuniformly dense trees were rejected. The remaining spectra were
separated into one of four categories depending on whether they were sunlit,
shaded, mineralized, or nonmineralized: 1) sunlit- nonmineralized, 2) sunlit-
mineralized, 3) shaded-nonmineralized, and 4) shaded-mineralized. The spectra
in each category were then averaged and compared. Figure 6a shows an average
of 10 sunlit - mineralized and 10 sunlit - nonmineralized spectra from flight
line #1. The mineralized spectra have higher reflected radiance values in the
visible portion of the spectrum. In the near infrared portion, the mineralized
reflected radiance values are also higher than the nonmineralized values, but
proportionally the difference is less. By dividing the mineralized by non-
mineralized spectra channel by channel, the two average spectra are compared
in a ratio plot (Figure 6b). The greatest proportional difference in the
average spectra occurs in the 0.67 µm region of the spectrum. The difference
is least in the 0.79 µm region. Eight flight lines, both morning and after-
noon, yielded sufficient numbers of spectra for 11 such ratio plots. Of
these 11 ratio plots, four compared sunlit spectra and seven compared shaded
spectra. Nine of the 11 plots showed the general properties depicted in Figure
6, i.e., higher 0.67 µm and near equal 0.79 µm reflected radiance values for
the mineralized spectra. Two ratio plots showed equal or lower 0.67 µm
reflected radiance values for the mineralized spectra, but equal values in the
0.79 µm region (Birnie and Hutton, 1976).

The experiment described above required prior knowledge of the zones of
mineralization; therefore, it does not provide an exploration tool. A method
of analyzing the spectra without prior knowledge of the geology has been
developed employing data representing an average of 12 spectrometer channels in
the 0.67 µm and 0.79 µm spectral regions. First, a flight line of data is
analyzed spectrum by spectrum to determine which spectra represent uniformly
dense vegetation; those spectra representing nondense vegetation such as roads,
grass, etc., must be removed. Spectra that do not represent uniformly dense
vegetation have anomalously high reflected radiance values in the 0.67 µm
region. Figure 7a shows a plot of the 0.67 µm reflected radiance values across
flight line #11. Those values that are associated with streams, roads, grass,
and nondense vegetation are indicated by a cross. All but one of these

"bad spectra" have reflected radiance values greater than 0.00125 mW/(cm^2.sr. channel). It is concluded, therefore, that it is possible to discriminate between dense vegetation spectra and other spectra by rejecting all spectra that have 0.67 μm reflected radiance values greater than a particular cutoff, in this case 0.00125 mW/(cm^2.sr.channel).

The dense tree spectra are separated into sunlit and shaded categories based on a discriminant at 0.79 μm where the effects of shading are emphasized by a relatively strong reduction in reflected radiance. It should be recalled that the effects of mineralization on the spectra are minimal in the 0.79 μm band. In Figure 8, the 0.79 μm reflected radiance values are plotted for flight line #11 with the sunlit and shaded zones indicated. If a cutoff is applied at the 0.00375 mW/(cm^2.sr.channel) and all spectra with reflected radiance values above and below this cutoff are considered sunlit and shaded, respectively, a good correlation with the ground truth is achieved.

Now it is necessary to discriminate between the mineralized and non-mineralized spectra within each of the shaded and sunlit categories. The ratio plot in the averaging experiment (Figure 6) indicates that the mineralization effects are most pronounced at 0.67 μm. Figures 7b and 7c show the 0.67 μm plots of reflected radiance values for the sunlit and shaded spectra, respectively. A cutoff can be applied to these data with all values greater than 0.0085 mW/(cm^2.sr.channel) in the sunlit zone and 0.0070 mW/ (cm^2.sr.channel) in the shaded zone classified as mineralized. In this example, most of the mineralized spectra are from a sunlit region; however, the same line was flown in the afternoon when the mineralized spectra were shaded, and a similar cutoff procedure isolated the mineralized zone within the shaded spectra.

If the zones of mineralized and nonmineralized spectra are recombined as in Figure 7d, a comparison can be made between the zone of mineralization as identified by the anomalous 0.67 μm reflected radiance values and the zone of mineralization identified by Miller et al. (1973). The correlation is good with two errors of omission within the mineralized zone and several errors of comission in the nonmineralized zone.

When the eight flight lines of data that traverse the Heddleston deposit are analyzed in a similar manner, the results plotted (Figure 9), and the zone of anomalous 0.67 μm spectra enclosed, it is seen that the anomalous spectra identify a zone that includes the shallow to intermediate depth mineralization but also extends beyond this zone. It is reasonable to expect that vegetation would manifest anomalous reflectance values beyond the zone of mineralization, because any soil geochemical anomalies would be expected to be dispersed beyond the border of the bedrock mineralization. The errors placing mineralized spectra outside the mineralized zone are particularly noticeable in the eastern part of the map. These erroneous spectra appear in areas where the vegetation is anomalously sparse.

While this method needs testing both in other mineralized areas and with other types of vegetation, the results of this study indicate that an airborne spectrometer measuring reflected radiance values of vegetation represents a potentially powerful exploration tool for the economic geologist.

REFERENCES

Birnie, R.W. and M.S. Hutton, 1976, Reflective spectra of vegetation growing over the Heddleston copper-molybdenum deposit, Montana (abs.): Abstracts with Programs, G.S.A. An. Meet., Nov. 1976, Denver, p. 779-780.

Collins, W., 1976, Spectroradiometric detection and mapping of areas enriched in ferric iron minerals using airborne and orbiting instruments: Ph.D. Dissertation, Columbia University.

Hunting Survey Corporation, Ltd., 1960, Reconnaissance Geology of Part of West Pakistan; a Colombo Plan Cooperative Project: Toronto, 550 p.

Miller, R.N., E.P. Shea, C.C. Goddard, Jr., C.W. Potter, and G.B. Brox, 1973, Geology of the Heddleston copper-molybdenum deposit, Lewis and Clark County, Montana: presented at Pacific Northwest Metals and Minerals Conference, Coeur d'Alene, Idaho, April 12-14, 1973.

Schmidt, R.G. and R. Bernstein, 1977, Evaluation of improved digital processing techniques of LANDSAT data for sulfide mineral prospecting: in Proc. First An. William T. Pecora Mem. Symp., Oct. 1975, Sioux Falls, U.S. Geol. Surv. Prof. Paper 1015, p. 201-212.
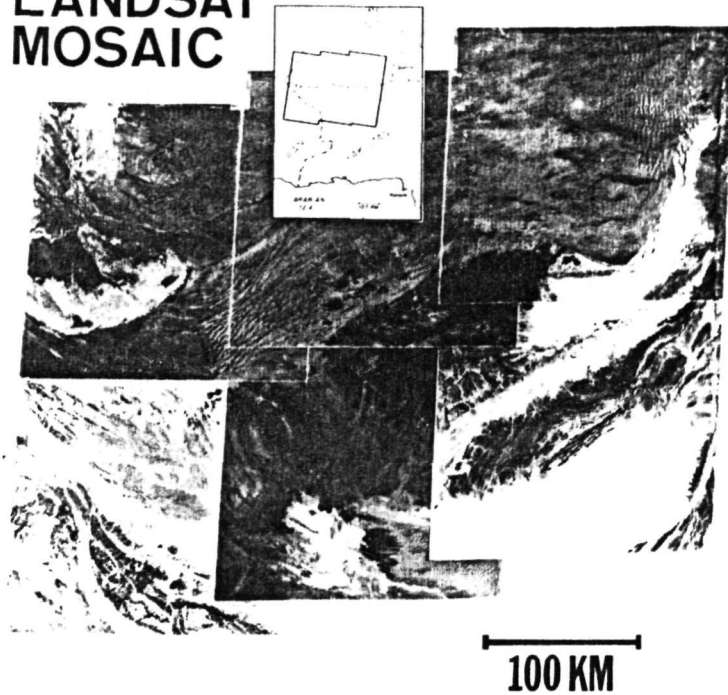
Figure 1. LANDSAT MOSAIC

Mosaic of six LANDSAT frames covering the study area. The
study area is that portion of Chagai Hills which is in
Pakistan (cross-hatched section of the eliptical feature
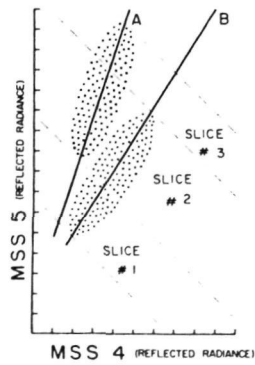in inset location map).

Figure 2. CHARACTERISTIC LINES

Distribution of pixels of two
hypothetical control areas
showing "characteristic lines"
(A+B) and lines of constant
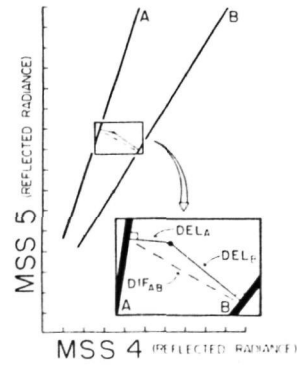total reflected radiance (dashed).

Figure 3. DIF AND DEL

An unknown pixel's (dot)
perpendicular distance from
each control area (DEL_A and
DEL_B) and the separation of
the two control areas (DIF_{AB}).

801

Figure 5. W. END OF CENTRAL LINEAR

Photo-geologic (a) and LANDSAT geologic (b) maps of the west end of the central linear of the Chagai Hills, Pakistan. The photogeology is by the Hunting Survey (1960). SjV=Sinjrani Volcanics, ChI=Chagai Intrusives (undifferentiated), ChI(a)= Chagai Intrusive granodiorite-quartz diorite, ChI(b)=Chagai Intrusive granite, Rec= volcanic float.

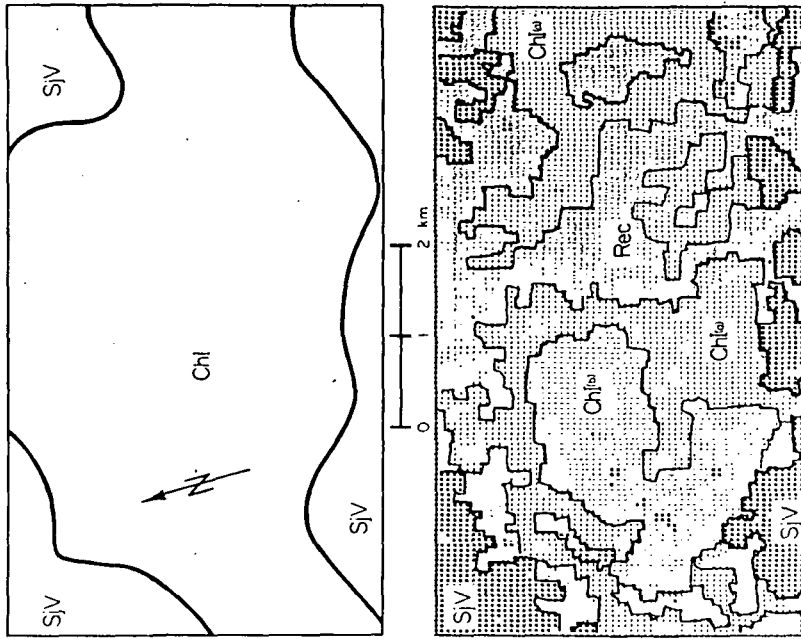Figure 4. E. END OF CENTRAL LINEA.

Photo-geologic (a) and LANDSAT geologic (b) maps of the east end of the central linear of the Chagai Hills, Pakistan. The photogeology is by the Hunting Survey (1960). SjV=Sinjrani Volcanics, ChI=Chagai Intrusives (undifferentiated), ChI(a)= Chagai Intrusive granodiorite-quartz diorite, ChI(b)=Chagai Intrusive granite, Rec= volcanic float.
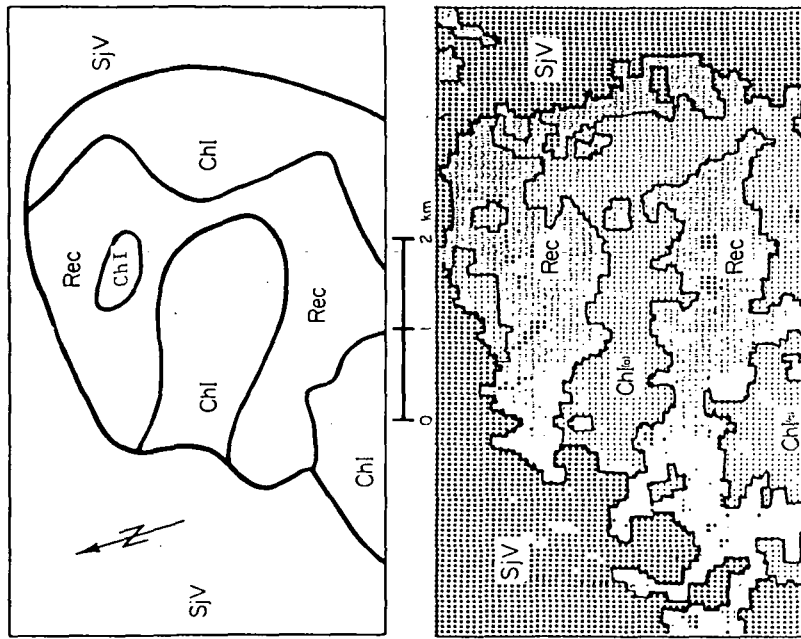
Figure 8. 0.79 μm VALUES

0.79 μm reflected radiance
values along flight line #11
west to east with shaded zones
shaded and sunlit/shaded
cutoff indicated as horizontal
line.

Figure 7. 0.67 μm VALUES

0.67 μm reflected radiance values
along flight line #11, west to
east, with mineralized zone
shaded: (a) All spectra with
nondense tree spectra shown as
X's and the nondense tree cutoff
indicated as horizontal line.
(b) Sunlit spectra only with
mineralization cutoff shown as
horizontal line. (c) Shaded
spectra only with mineralization
cutoff shown as horizontal line.
(d) Recombination of (b) and (c)
with mineralized spectra on
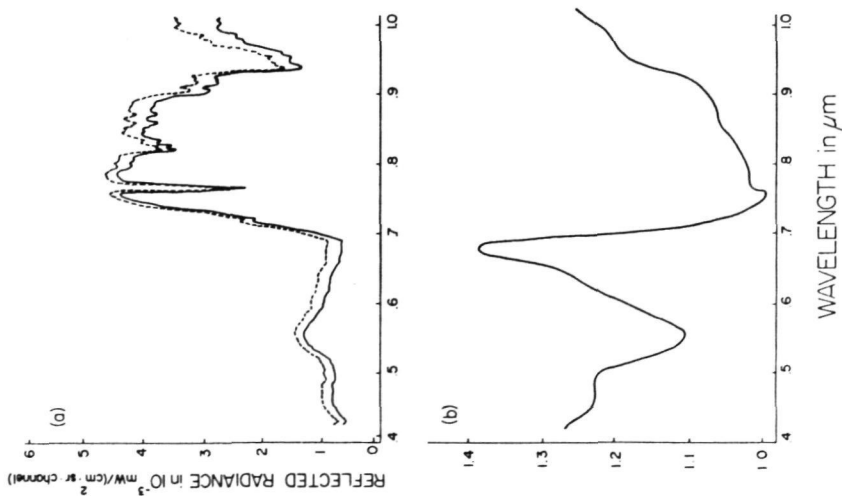upper line and nonmineralized
on lower line.

Figure 6.
AVERAGED SPECTRA AND RATIO PLOT

(a) The average of 10 "miner-
alized" spectra (dashed line)
and 10 "nonmineralized" spectra
(solid line) for flight line
#11. (b) Channel by channel
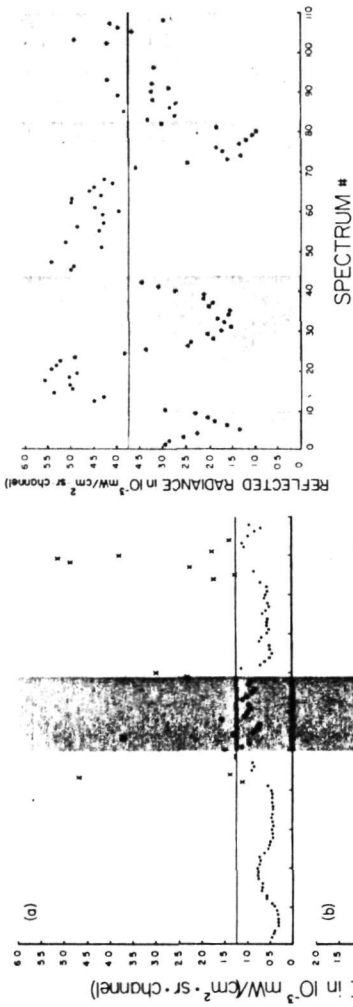ratio plot of mineralized/
nonmineralized spectra.

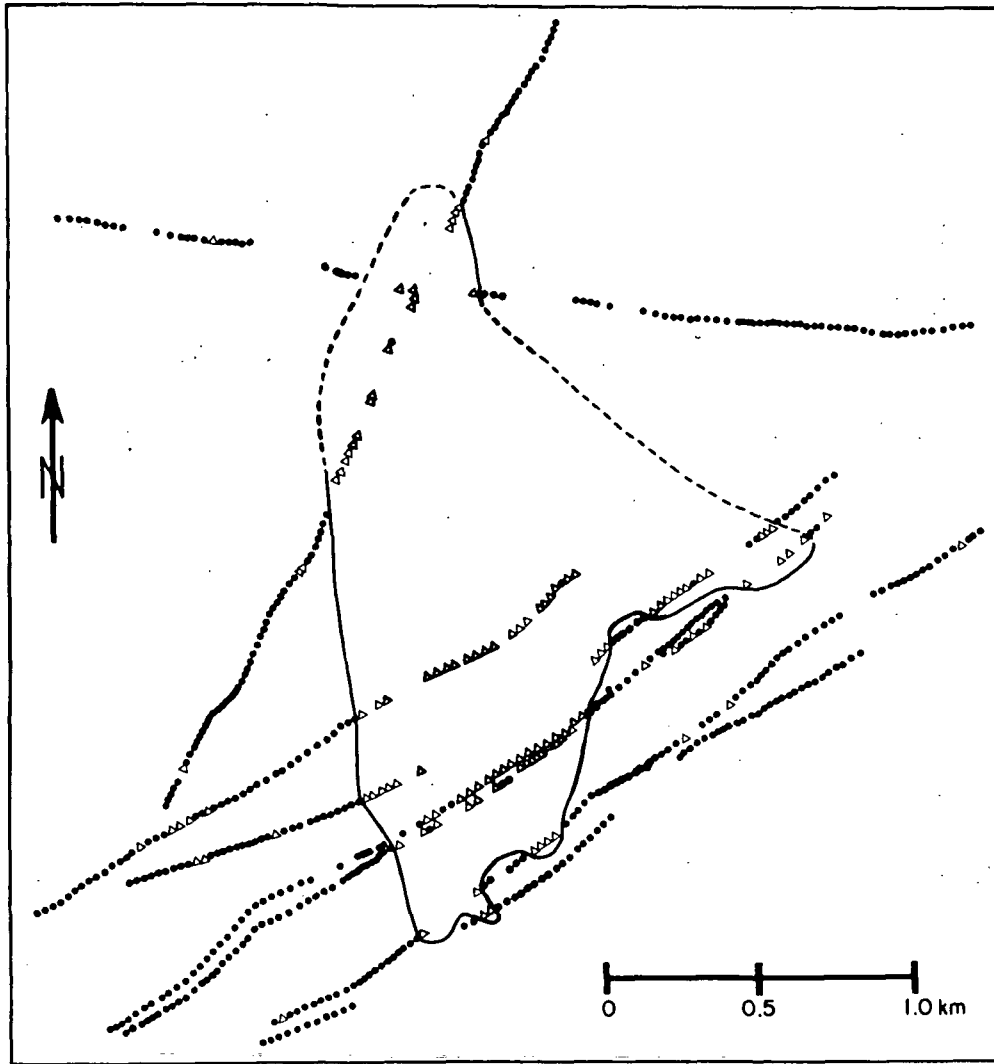Figure 9. MAP OF MINERALIZATION AND ANOMALOUS SPECTRA

The zones of shallow to intermediate depth mineralization
at the Heddleston deposit are indicated by shading (after
Miller et al., 1973). Traces of individual flight lines
are shown with spectra classified as mineralized and
nonmineralized indicated by open triangles and dots
respectively. The solid bold line interprets the
mineralized zone from the spectral data.

IV, and by local contact ion exchange in VI, suggesting presence of pervasive fluid in I-IV, but absence in VI, consistent with features of cataclasites in these zones.

LONG-DISTANCE CHRONOCORRELATION IN THE MIDDLE CAMBRIAN
    Robison, R. A., Department of Geology, University of Kansas, Lawrence, Kansas 66045; McGee, J. W., Cities Service Oil Company, Box 300, Tulsa, Oklahoma 74102; Rowell, A. J., Department of Geology, University of Kansas, Lawrence, Kansas 66045; Strickland, D. K., Department of Geology, University of Kansas, Lawrence, Kansas 66045; and White, W. W., III, U.S. Bureau of Land Management, Buffalo Resource Area, Buffalo, Wyoming 82834.
Most Cambrian species are endemic, which creates severe problems in global chronocorrelation. The majority of agnostoid trilobites were probably pelagic and some were cosmopolitan. Two species, Ptychagnostus gibbus and P. atavus, show widespread stasis throughout their geographical range, but both are separated by morphological gaps from their putative ancestors. Their phylogeny is consistent with a punctuated-equilibrium model of speciation.

The bases of both the P. gibbus and P. atavus zones have previously been suggested as potential horizons for series boundaries. In many parts of the world the incoming of P. gibbus is associated with a marked change in lithology, and in detail, the initial appearance of the species may have been delayed at any given locality. In contrast, P. atavus commonly occurs in monofacial open-ocean successions and probably its initial appearance closely followed speciation. In western Utah, a likely area for establishment of a series boundary-stratotype, P. gibbus and other trilobites occur with inarticulate brachiopods in the lower part of the Wheeler Shale, which accumulated under relatively deep-water conditions. Without significant change in either lithology or the inarticulate brachiopod assemblage, P. gibbus is abruptly replaced by P. atavus. Associated changes in polymeroid trilobites, although less extensive, resemble changes at the bases of Late Cambrian biomeres, which have been interpreted as adjustments to cooler water. Considering all factors, chronocorrelation based on the first appearance of P. atavus is probably as precise as any in the Cambrian.

TRACE ELEMENT GEOCHEMISTRY OF MAFIC AND FELSIC MINETTES, BUELL PARK DIATREME, NAVAJO VOLCANIC FIELD
    RODEN, Michael F., Department of Earth and Planetary Sciences, Massachusetts Institute of Technology, Cambridge, Massachusetts 02139, and Department of Geological Sciences, University of Texas, Austin, Texas 78712
Potassium-rich minettes (3.5-7% K_2O, $K_2O > Na_2O$) of the Navajo volcanic field containing abundant spinel and rarer garnet lherzolite inclusions were erupted 25-30 million years ago in the central Colorado Plateau. Samples of mafic (49% SiO_2, 10% MgO) to felsic (60% SiO_2, 4% MgO) minette from the Buell Park composite kimberlitic breccia-minette diatreme were analyzed for rare earth elements (REE), Rb, Ba, Sc, Cr, and Ta by instrumental neutron activation. Chondrite-normalized REE patterns for all the minettes are similar and highly fractionated (La = 330-370 x chondrite, Yb = 5-7 x chondrite). Also, Ba increases slightly through the suite (2100-2350 ppm), while Rb increases by two-fold (100-200 ppm). In contrast, compatible elements decrease significantly from mafic to felsic minette: Cr, 410 to 100 ppm, and Sc, 16 to 9 ppm. A major element model based on whole rock and phenocryst analyses relates mafic to felsic minette by fractionation of diopside, phlogopite, magnetite, and apatite. Apatite fractionation was important in controlling the REE and explains decreasing P_2O_5 and P_2O_5/Ce through the suite. The fractionation of Cr and the "buffering" of the REE are not easily explained by a model in which mafic and felsic minette are derived by different amounts of partial melting of the same source. P_2O_5/Ce ratios ($\simeq 40$) of mafic minettes are lower than that suggested for the source of alkali basalts and nephelinites and are consistent with a source for the minettes enriched in light REE. A garnet lherzolite which initially contained apatite and phlogopite is a possible source.

HYDROTHERMAL TRANSPORT AND DEPOSITION OF URANIUM, AND THE ORIGIN OF VEIN URANIUM DEPOSITS.
    ROMBERGER, Samuel B., Department of Geology, Colorado School of Mines, Golden, Colorado 80401.
The stabilities of various aqueous uranium complexes are evaluated at up to 300°C using available thermodynamic data. The distribution of aqueous uranium species are plotted as a function of pH and log oxygen fugacity to determine the complexes responsible for the transport, and the mechanisms for deposition, of uranium in natural hydrothermal systems. When these results are considered along with the hydrothermal alteration and mineral assemblages observed in vein uranium deposits, the following conclusions are reached: 1) Carbonate complexes become less important at elevated temperatures and are not significant in the transport of uranium in hydrothermal systems. 2) In deposits containing fluorine, uranyl fluoride complexes are most important in uranium transport. 3) Chloride complexing is not significant even where chloride activities exceed 1. 4) Under certain conditions phosphate complexing may be important in transporting uranium. 5) The solubility of pitchblende decreases as temperature increases, and therefore cooling is not an adequate mechanism for deposition. 6) Uranium is deposited by an increase in pH or a decrease in activity of complexing anions. These changes may occur as a result of reaction with wall rocks, boiling and loss of volatile components, or mixing with ground waters. 7) Oxidation of iron in wall rocks may be an effect of, rather than a cause for, uranium precipitation. 8) Pitchblende can precipitate under conditions where pyrite or hematite are stable, or where iron is mobile, resulting in the bleaching of wall rocks.

LARGE-SCALE "GRENVILLE" NAPPE STRUCTURES INVOLVING GRANITIC GNEISSES IN SOUTHEASTERN ONTARIO AND THE NORTHWEST ADIRONDACK LOWLANDS
    ROMEY, Bill and JACOBY, Russell S., Department of Geology and Geography, St. Lawrence University, Canton, N.Y. 13617
A competent, rumpled, northwest-dipping sheet of granitic gneiss extends from Parishville to Alexandria Bay, N.Y. Apparently isolated leucogneisses (the Canton, Gouverneur, Hyde School, Fish Creek, California, Clark Pond, and other "phacolithic" bodies) result from "egg-carton" structure of the sheet. Contorted, plastically deformed, incompetent metasedimentary rocks fill troughs and depressions between domal axial culminations on the granitic sheet.

Structural relationships show the Parishville body, to the east, as the hinge of a major, recumbent, isoclinal nappe, with one limb extending into the Adirondack Highlands. To the west, the granitic gneisses at North Hammond and Alexandria Bay extend the sheet across the St. Lawrence River to include the Rockport granite in Ontario, possibly forming another major fold hinge. The amplitude of these folds approaches 60 miles. They extend a competent granitic stratigraphic unit across the southwestern part of the Grenville Province. The northeast-trending "grain" of Grenville structures represents axial-surface foliations to these nappes.

Granitic rocks of the sheet may represent metasediments or metavolcanics of the Grenville Supergroup which have locally undergone melting and remobilization. Other acidic gneisses beyond the ends of the fold hinges, such as charnockitic gneisses of the Diana and Santa Clara complexes, New York, may be correlative with the Westport, Crow Lake, Gananoque, Lyndhurst, and Perth Road metaplutonic bodies in Ontario and therefore represent rocks derived from anatexis of pre-Grenville basement rocks.

EARLY CENOZOIC PLATE REORGANIZATION
    RONA, Peter A., and RICHARDSON[1] Evan S., National Oceanic and Atmospheric Administration, Atlantic Oceanographic and Meteorological Laboratories, Miami, Florida 33149
    [1]Also University of Miami, Rosenstiel School of Marine and Atmospheric Science, Miami, Florida, 33149

Synthesis of regional plate movements reveals a major reorganization of global plate motion from Mesozoic to Cenozoic patterns that occurred primarily during the Eocene epoch (53.5 to 37.5 my BP). The reorganization involved reorientation of relative plate motions with large N-S components into large E-W components, continuation of pre-existing E-W sea floor spreading, initiation of new E-W spreading, deceleration of spreading rates, and obduction of ophiolites. The reorganization is attributed to increase in resistance imposed on the global plate system by increase in length of E-W trending collisional plate boundaries from 2,500 to 28,500 km during the interval 55 to 40 my BP, forcing the system to reorient along lines of less resistance. The pattern of global plate motion resulting from the reorganization is constrained by the resistance imposed by 19,000 km of collisional plate boundaries.

BIOTURBATE TEXTURES IN MUDDY SEDIMENTS
    RONAN, Thomas E. Jr., Department of Earth & Space Sciences, University of California, Los Angeles, California 90024; LIPPS, J. H., Department of Geology, University of California, Davis, California 91567

The textural properties of muddy sediments are influenced to a large degree by the motility modes and feeding types of their resident biota.

A muddy sediment which contains a dense assemblage of suspension feeding infauna which build tubes will have a bioturbate texture that arises primarily from the activity of its between-the-tubes community. Myriad small sinuous burrows, primarily produced by annelids and crustaceans, will pervade the sediment. Because the tubes constitute a barrier to subsurface locomotion, the large resident skeletonized infauna (bivalves and shrimp) will consist of relatively sessile species that build permanent burrows. The overall effect is to produce a sediment that is cohesive and contains well-defined biogenic structures. Because cemented tubes tend to degrade quickly, paleontologic recognition of a tube-builder association may depend entirely upon the distinctiveness of the suite of sediment traces produced by the coexisting infauna.

By comparison, a less densely populated muddy sediment will have a bioturbate texture that results from deposit feeding and locomotion traces. The active probing of sediment with tentacles, proboscis, and palps will produce a mottled to homogenous sediment texture. The overall water content of this sediment will be high and deformation of biogenic structures would be expected during preservation.

1978 VOLCANIC ERUPTION CLOUD SAMPLING PROJECT
    ROSE, W. I., Jr., CADLE, R. D., LAZRUS, A. L., HEIDT, L. E., and D. A. GILLETTE, National Center for Atmospheric Research, Boulder, CO 80307; HUEBERT, B. J., Colorado College, Colorado Springs, CO 80903;

1978 Joint Meeting (GSA, Geological Assoc. of Canada) Toronto Oct 24-26, 1978.

Encl 4

STOIBER, R. E., SELF, S. and BRATTON, C., Dartmouth College, Hanover, NH 03755; CHUAN, R. L., Brunswick Corporation, Costa Mesa, CA 92626; WOODS, D. C., NASA Langley Research Center, Hampton, VA 23665; FRIEDMAN, I., ZIELINSKI, R. A. and SMITH, D., U.S. Geological Survey, Denver, CO 80225; WILSON, L., University of Rhode Island, Kingston, RI 02881.

During February and March 1978, a team of scientists and a specially equipped Queen Air Aircraft flew eleven sampling flights over the active volcanoes of Pacaya, Fuego and Santiaguito in Guatemala. Throughout this period each of the volcanoes showed moderate activity and had plumes which could be readily sampled at various altitudes and distances from the active craters.

Equipment on the aircraft included: 1) a treated filter sampler for determination of relative amounts of SO_2, HCl, HBr, HF, $SO_4^=$, particulates and trace elements; 2) a 10-stage Piezoelectric Particle Cascade for particulate size distribution and size sampling of particulates in the range of 25 to 0.05 μm; 3) evacuated stainless steel canisters for quantitative gas chromatographic measurements of H_2S, COS, CO_2, CO and SO_2; 4) a SO_2 correlation spectrometer for the determination of SO_2 fluxes in the plumes by traversing; 5) an automatic 35 mm multi-speed sequence camera for dynamic photography of erupting plumes; 6) a flow-thru stainless steel gas sampler for H, O and C isotopic measurements of gases; 7) an Inertial Navigation System for ground and wind speed determinations; 8) a gas bubbler sampler for trace element sampling. At abstract time, few results are available.

The project demonstrates clearly the feasibility of planned missions to sample more or less continuous low level emission from the same explosive volcanoes that project material into the stratosphere in short-lived sporadic events.

SNOWBALL MUSCOVITE IN THE CENTRAL SWISS ALPS: AN INTERNAL RECORDER OF TECTONOMETAMORPHISM
Rosenfeld, J. L., Department of Earth & Space Sciences, University of California, Los Angeles, California 90024
Snowball muscovite (SM) occurs with the well-known snowball garnet (SG) in north-dipping, staurolite-zone, Liassic calcareous schists in the isoclinal Piora Syncline separating the Gotthard and Lucomagno massifs. Its lower symmetry causes SM to reveal petrogenetic features beyond those shown by SG. Some muscovite recrystallized around new nuclei of scattered orientation while other coexisting muscovite reacted to form snowball biotite. Rotation of SM and their simultaneous, orientation-dependent, anisotropic growth-rate caused changes in cross-sectional shapes normal to their rotational axes from relatively equant [(001)~+foliation (S)]to elongate || (001)[(001)~||S]. Low angular velocity in the latter state kept S parallel to the synclinal axial surface (cf. D. Willis). Garnet pseudomorphs of muscovite, including earlier SM, demonstrate muscovite translocation by cation exchange, probably along intergranular boundaries influenced by differences in surface energy and changing phase equilibrium. SM, SG, and other snowball minerals show rotational sense that is invariant with position in the syncline. Their south-side-up sense indicates growth during Chadwick's tectonic Phase V after folding of the Piora Syncline. That shear, with elongation parallel to the dip (e.g. boudinage of zoisite during growth), probably derived from Oligocene southward tilting of the bordering, more competent massifs, caused by southward slumping of material at a higher crustal level. That movement also accounts for refolding of nappe-related isoclinal folds in the Triassic dolomite at nearby Passo Campolungo.

ECOLOGY OF LARGER, SHALLOW-WATER TROPICAL FORAMINIFERIDA
ROSS, Charles A., Department of Geology, Western Washington University, Bellingham, Washington 98225
Modern coral reefs are inhabited by a great abundance and diversity of species of Foraminiferida. On exposed reef flats and exposed shallow intra-reef basins species of Calcarinidae and Amphisteginidae dominate the Thalassia (turtle grass) blades and may form the substrate of the basins, the upper surfaces of which are bound together by foraminiferal pseudopods. Although most of these species are relatively small, the families Soritidae and Alveolinidae have representatives that reach shell volumes greater than 100 mm. The soritid Marginopora vertebralis occurs abundantly in a number of different reef environments, including clinging to Thalassia blades in 1 to 2 m deep protected lagoons. M. vertebralis and other larger foraminiferids start to appear consistently on substrates composed of smaller foraminiferids in deeper intra-reef basins 8 to 25 m deep on exposed reefs, and inter-reef channels about 25 m deep. Growth rate decreases but the final size necessary to reach reproductive maturity increases below a depth of 10 m, so that the largest specimens are from the deeper locations.

The shallow depth limits in the distribution of large reef-dwelling foraminiferids are related to exposure to waves and currents that are of sufficient strength to displace the foraminiferids and redeposit them in deeper water. The lower depth limits, at least for the soritids, are related to the depth at which their photosynthetic zooxanthellae partners are no longer effective symbionts.

ASBESTOS HEALTH RISKS TO THE MINING COMMUNITIES OF NORTH AMERICA
ROSS, Malcolm, U.S. Geological Survey, 959 National Center, Reston, Virginia 22092

Mesothelioma, a cancer of the pleura and peritoneum, occurs, with few exceptions, only in asbestos "trades" workers (ship insulation, textiles, construction, etc.) and in South African crocidolite miners. Lung cancer is seldom found in non-smoking asbestos "trades" workers. The percent mortality for lung cancer and mesothelioma is plotted for 11 groups of "trades" workers. Regression analysis of these data shows a linear relationship between lung cancer and mesothelioma incidence; 79% of the variance (r^2) of lung cancer is accounted for by mesothelioma. A large part of the remaining 21% variance can be accounted for by intergroup differences in smoking statistics. Cancer mortalities are also plotted for adult male populations of 5 nations and for 6 "asbestos" mining/factory populations not exposed to crocidolite. The very low incidence of mesothelioma in these groups shows that they do not have the cancer risk experienced by those in the "trades"; their lung cancer incidence is generally accounted for by smoking habits alone. Cancer risk to those in the "trades" is attributed to exposure to both smoke and crocidolite. There is no evidence that the mineral dust levels presently maintained in responsibly operated mines of North America cause increased incidence of lung cancer or mesothelioma, including those mines that process rock containing the commercial forms of asbestos: anthophyllite, tremolite, actinolite, cummingtonite, grunerite, and chrysotile.
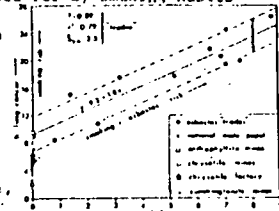
THE DFE PROGRAM IN ENVIRONMENTAL IMPACT OF THE DISPOSAL OF HIGH LEVEL RADIOACTIVE WASTE IN GEOLOGICAL FORMATIONS
Rothschild, H. C. and Barraud, C., Nuclear Programs Division, Department of Fisheries & Environment, Ottawa, Ontario, K1A 1C8.
Fisheries & Environment Canada's interest in the problem of disposal of high level nuclear wastes in geologic formations involves the participation of two services: Environmental Management Services (EMS) and Environmental Protection Services (EPS). EMS is supporting applied research in hydrogeology and groundwater geochemistry for determining the transport/retardation mechanisms of radionuclides in the sub-surface environment. The EPS involvement consists of preparing a document providing recommendations for long-term protection of our environment with respect to disposal of high level radioactive waste. This document will cover two main topics:

(a) evaluation of long-term physical and chemical stability of the different rock types considered to be potentially suitable as high-level waste disposal media.
(b) evaluation of the efficiency of the geologic barrier for long-term containment of long-lived radionuclides.

Conclusions drawn from this document will provide a base for recommending improvement of solidification techniques to produce synthetic matrices with long-term physical and chemical stability and with lower leaching rates than the present day glass or ceramic matrices.

DEVELOPMENTAL CYCLE AND SYMBIOSIS OF THE RECENT NUMMULI-TID, HETEROSTEGINA DEPRESSA, AND THEIR IMPLICATIONS FOR THE OCCURRENCE OF THE MICROSPHERIC GENERATION
RÖTTGER, Rudolf, Institut für Allgemeine Mikrobiologie der Universität Kiel, Olshausenstr. 40-60, 2300 Kiel, Fed. Rep. of Germany
The developmental cycle of Heterostegina depressa has been investigated in laboratory cultures and in specimens from natural habitats in Hawaii. As in other foraminiferan species, alternation of generations also exists. However, megalospheric specimens (gamont, A-form) are much more abundant than microspheric specimens (agamont, B-form). This seems to be true for all larger foraminifera (Recent and fossil). The reason for this is that multiple fission is the main mode of reproduction of the megalospheric generation. Gamete formation, which leads to the microspheric generation, is greatly reduced. The symbiotic diatoms which are essential for the metabolism of this foraminifer are easily transferred over many megalospheric generations during multiple fission. Gamets, which are rarely formed by megalospheric individuals, do not transfer symbionts to the microspheric generation. Consequently, the microspheric generation has to engulf free living diatoms during its early individual development and transform them into symbionts. The transformation process makes the establishment of symbiosis more difficult in the microspheric generation. Such difficulties along with the scarcity of gamete formation may account for the small number of microspheric specimens found in natural habitats and for their special depth distribution. Microspheric specimens occur to a depth of 100 m with the highest frequency in the deeper regions of this range.

THE PAST AS A KEY TO THE PRESENT: PLANKTONIC FORAMINIFERA AND PTEROPODS IN SOUTH CHINA AND JAVA SEA SEDIMENTS
ROTTMAN, Marcia L., Department of Geology, Humboldt State Univ.,

punted by lava flows and explosive vulcanian activity. During our sampling, Pacaya was in a state of intense vapor emission which began in December 1977 and continued at least through May 1978. Little or no ash was being erupted, and no lava flow activity was occuring either. When vapor emission abated during our sampling flights, magma could be directly observed through gashes within the McKenny crater. Fuego has departed from its 20-year pattern of short-lived, frequent, violent pyroclastic eruptions. Beginning in September 1977 and continuing until at least June 1978, Fuego has been in constant low-level pyroclastic activity. In February 1978, lava flows, the first since at least 1932 at Fuego, were flowing down the SW flank of the cone. Larger lava flows were seen in the E flanks in June. Mild vulcanian activity producing substantial amounts of ash was interspersed with vaporous, ash-poor plumes in February. Both types of eruption clouds were sampled. Santiaguito is a Pelean dome, which has been continuously erupting since 1922. Since April 1975 the volcano has been producing several pyroclastic eruptions each day, some reaching heights ~5 km. During February this activity continued to produce large, ash-rich eruption clouds. Continual, relatively low level activity at ever-changing subsets of Central America volcanoes allow planned missions to sample explosive volcano clouds at small (<4000 m) volcanoes in good (dry season) weather conditions.

*NCAR is sponsored by the National Science Foundation.

V 74 INVITED PAPER

SULFUR AND HALOGEN CONSTITUENTS OF VOLCANIC ERUPTION CLOUDS

A. L. Lazrus
R. J. Huebert
R. D. Cadle (all at: National Center for Atmospheric Research, Boulder, CO 80307*)
W.I. Rose, Jr. (Michigan Technological University, Houghton, MI 49931)

Volcanic plumes in Guatemala and Alaska were sampled for SO_2, HCl and HF vapors as well as SO_4, Cl^- and F^- in particles. The molar ratios for SO_2/HCl varied from 1.2 to 7.5, and that of HCl to HF from 5 to 71. Selective removal of HCl and HF with respect to SO_2 as a function of distance from the crater was not observed. The average percentages of sulfur, chlorine and fluorine in the particle phase are respectively 2.5, 18 and 42.

The amount of sulfate present in the northern hemisphere stratosphere in Spring 1975 resulting from the Fuego eruption in Fall, 1974, has been estimated from isopleth maps of sulfate concentration obtained by means of WB57f aircraft and balloons.

V 75 INVITED PAPER

AIRBORNE CORRELATION SPECTROMETER MEASUREMENTS OF SO_2 IN ERUPTION CLOUDS FROM GUATEMALAN VOLCANOES

Richard E. Stoiber
G. Bratton (both at: Dept. of Earth Sciences, Dartmouth Coll., Hanover, NH 03755)

Measurements of SO_2 emitted during mild eruptions of the Guatemalan volcanoes Fuego and Santiaguito emitted in a strong vapor cloud at Pacaya were made with an airborne remote sensing correlation spectrometer. Emission of 300 to 1500 metric tons per day of SO_2 is comparable with data from ground-based measurements made at other times and at other volcanoes elsewhere. The airborne mode eliminates the necessity of roads being positioned appropriately relative to the plume; and allows many traverses to be made beneath the plume in a short period of time. These traverses may be at any desired distance below the plume or downwind from the crater. Thus one can investigate the change in SO_2 in the plume downwind as well as the instrument response at various distances beneath the horizontal plume due to vertical distribution of the gas and to atmospheric attenuation. Measurements indicate attenuation loss of at least 20% in the signal from a plume where it is 1.8 km above the aircraft and a marked drop of up to

40% in SO_2 content downwind at distances of up to 25 km from the volcanic crater. Use of the spectrometer in an aircraft requires appropriate navigational aids and an exit port for the telescope with no overhead obstructions.

V 76 INVITED PAPER

GAS AND H ISOTOPIC ANALYSES OF VOLCANIC ERUPTION CLOUDS IN GUATEMALA

W. I. Rose, Jr.
R. D. Cadle
L. E. Heidt
R. J. Huebert
A. Lazrus (all at: National Center for Atmospheric Research, Boulder, CO 80307*; pres. address (Rose): Michigan Technological University, Houghton, MI 49931)
I. Friedman (U. S. Geological Survey, Denver CO 80225)

Gas samples were collected by aircraft entering volcanic eruption clouds of three Guatemalan volcanoes. Gas Chromatographic analyses show higher H_2 and S gas contents in ash eruption clouds and lower H_2 and S gases in vaporous gas plumes. H isotopic data demonstrate lighter isotopic distribution in water vapor of ash eruption clouds than in vaporous gas plumes. Most of the H_2O in the vaporous plumes is probably meteoric. The data are the first direct gas analyses of explosive eruption clouds, and demonstrate that, in spite of atmospheric admixture, useful compositional information on eruptive gases can be obtained using aircraft.

V 77 INVITED PAPER

PARTICLE SIZE DISTRIBUTION AND MORPHOLOGY OF ASH IN THE FUEGO AND SANTIAGUITO PLUMES

Stephen Self (Dept. of Earth Sciences, Dartmouth College, Hanover, NH 03755)

Airborne collection of pyroclastic particulates in the plume of Fuego and Santiaguito Volcanoes, Guatemala was conducted in February 1978. Particles were collected on both Fluoropore filters and on a quartz crystal microbalance (QCM) cascade impactor between 12 and 15,000 ft. above sea level and at various distances downwind. SEM examination of particles shows size range, particle type and morphology. Solid particles in the plume are juvenile scoria, crystal fragments and comminuted non-juvenile lithic material. Sizes range from 1mm to <0.05μm and the progressive downwind decrease of the coarse fragment content can be documented. This is compared to plume dynamics obtained from movie film of the explosions which produced the ash contained in the plume. Initial plume velocities of ~10 m/s, which decelerate dramatically to a few meters per second before being blown downwind, supported particles <25 um up to distances of ~15 km from Fuego Volcano with bulk concentrations of several thousand μg/m³. Data will also be presented on the relative concentration of the various particle types and the total grain size distribution in an eruption plume produced by mild vulcanian explosions.

V 78 INVITED PAPER

SIZE DISTRIBUTION, MORPHOLOGY AND ELEMENTAL COMPOSITION OF FINE PARTICLES IN VOLCANIC PLUMES

D. C. Woods (NASA Langley Research Center, Hampton, VA 23665)
R. L. Chuan (Brunswick Corp., Costa Mesa, CA 92626)
(Sponsor: R. D. Cadle)

Fine particles (from about 50 to 0.05 micrometers in diameter) in the eruption plumes from two active volcanoes, Fuego and Santiaguito, were sampled in situ to determine mass concentration and size distribution, with elemental composition and morphology determined from post sampling analysis. The samples were taken during an aircraft sampling mission in Guatemala in February and March 1978. The particles were

sampled with a 10-stage cascade impactor which has piezoelectric crystals as active collectors that produce, in real time, electronic signals corresponding to the mass of material deposited on the collector surface. The samples were photographed and analyzed in a scanning electron microscope equipped with an energy dispersive x-ray analysis attachment to determine elemental composition. The particles appeared to be divided among two morphological groups, large agglomerates in the large size fractions and less agglomerated particles in the small size fractions, giving the overall size distribution a bimodal character. Mass densities of the particles were estimated from their geometric sizes as seen in the SEM. The large agglomerates were estimated to have mass densities less than $2g/cm^3$ while the singlets have mass density of about $2g/cm^3$. Supporting data from another sensor on board the aircraft indicate that most of the particles are liquid crystal, presumably HCl and H_2SO_4. Energy dispersive x-ray analysis reveals significant amounts of Al, Si, S, Ca and Fe with lesser amounts of Cl, K and Ti in the large agglomerates and Al, Si, Fe and Ti in the submicron groups.

V 79 INVITED PAPER

VOLCANIC EXPLOSION PLUMES: DENSITY, TEMPERATURE AND PARTICLE CONTENT ESTIMATES FROM PLUME MOTIONS

L. Wilson (Environmental Science Dept., Univ. of Lancaster, Lancaster LA1 4YR, U.K.)
S. Self (Dept. of Earth Sciences, Dartmouth College, Hanover, N. H. 03755)

Analyses are reported of 7 eruption clouds from Fuego, filmed at one frame per second on February 27, 1978, as part of NCAR's Central American Volcano Plume Sampling Experiment. The movement of a cloud between frames gives its velocity. The velocity/time curve can be differentiated to find the acceleration and hence the total force acting on the cloud. This force consists of 2 parts, air drag (most important at high speeds early in the motion) and buoyancy (most important late in the motion when the cloud is convecting slowly). Equations of motion were derived for 2 common cloud shapes, spheres and vertical cylinders, and cloud densities were calculated by fitting the equations to the observed motions. A simplified analysis of the heat budget of a cloud permits an estimate of cloud temperature and particle weight fraction to be made from the density. Clouds generally reached temperatures within 10° of that of the surrounding air within 10 seconds of formation. Dense particle weight fractions were less than 2% by this time, and cloud rise velocities less than 5 m/s. In 4 cases it was possible to estimate the maximum size of dense particles supported by the cloud motion: values found were 315, 700, 140, and 560 microns.

V 80 INVITED PAPER

TRACE METALS IN VOLCANIC ERUPTION CLOUDS

D. B. Smith
R. A. Zielinski (both at U.S. Geological Survey, Denver, Co. 80225)
(Sponsor: C. W. Naeser)

In February and March of 1978 filter samplers mounted on an aircraft were used to collect the aerosol fraction of the eruption clouds of three active Guatemalan volcanoes (Fuego, Pacaya and Santiaguito). The filter sampler consisted of three filters in series. The first was a Fluoropore filter with a nominal pore size of 0.5 microns for removing particulates from the eruption cloud. The next two filters were Whatman filters treated with tetrabutyl ammonium hydroxide to preferentially retain acidic volatiles contained in the cloud. The mass of air sampled by the filters ranged from .15 to 6.6 km. For each volcano samples were collected at increasing distances from the vent. After collection of the samples, each filter was extracted with 60 ml of water. Splits were filtered and analyzed for 19 metals by inductively coupled plasma-optical emission spectrometry. Fluoride and chloride were analyzed by specific ion electrode.

The elements found in significant concentrations in the Fluoropore extracts are as follows (in decreasing order of concentration): Si, Ca, Fe, Mg, Cl, Na, F, Mn, Zn, V, Pb, Cu, Sr and Cd. These elements represent components of water-soluble sublimates derived from interaction of particulates and acidic gases of the eruption cloud. Elements found in the extracts of the

1978 Fall Meeting AGU, San Francisco Dec 4-8, 1978

Encl 5